# Chapter 2

# Surface Plasmon Resonance Biosensor for Biomolecular Interaction Analysis Based on Spatial Modulation Phase Detection

**Xiang Ding, Fangfang Liu, and Xinglong Yu**

## Summary

Surface plasmon resonance (SPR) biosensor is a powerful tool for biomolecular interaction analysis in proteomics research and drug discovery. But when it is used to analyze small molecules, the sensitivity still needs enhancement. Phase detection is a potential solution, for phase changes more abruptly than intensity when SPR is excited. An SPR system is developed based on spatial modulation phase detection (SMPD). In this system, collimated monochromatic light is used to excite SPR, and the phase of the reflected light is spatially modulated to generate an interference pattern. By processing the interference pattern by certain algorithms, instantaneous phase distribution of the whole sensing area can be obtained. Continuously detecting the phase change, the whole process of biomolecular interaction can be recorded in the form of phase change, based on which we can make kinetic analysis and get kinetic parameters. Antibody array chip is tested by this system. Experimental results indicate that this technique is capable of array detection and is more sensitive than intensity detection.

**Key words**: Surface plasmon resonance (SPR), Spatial modulation, Phase detection, Biomolecular interaction, Antibody array.

## 1. Introduction

Present commercialized surface plasmon resonance (SPR) biosensors are mostly based on intensity detection, which takes an advantage of simple system configuration. But due to drifts of the light source, the photoreceiver, and the amplification circuit, the detection precision is degraded, commonly no better than $10^{-6}$ refractive index unit (RIU).

Avraham Rasooly and Keith E. Herold (eds.), *Methods in Molecular Biology: Biosensors and Biodetection, Vol. 503*

DOI: 10.1007/978-1-60327-567-5_2

In proteomics research and drug discovery, the voice for techniques of small molecule detection is getting louder and louder. Small molecules are usually defined as those whose molecular weights are below several hundred Daltons. When interacting with other molecules, they generate very limited refractive index change, which is difficult to be detected. So it is necessary to enhance the sensitivity of SPR biosensing techniques. There are two solutions: one is to modify the analyzed molecules, for example, nanoparticle modification; the other is to excavate the potential of sensors. As we know, modification to molecules may lead to a lot of problems: poor repeatability, time wasting, influence on molecular activity, etc. An approach to higher sensitivity without modification to molecules is preferable. When SPR is excited, both the reflected light's intensity and phase vary rapidly, but the phase changes much more abruptly than the intensity. It means that detecting phase of the reflected light instead of its intensity is a simple way to enhance the sensitivity of SPR biosensor. Theoretical analysis indicates that the sensitivity of phase detection is higher than that of intensity detection by 1–2 magnitudes *(1)*.

There are many phase detection techniques, including ellipsometry, interferometry, and heterodyne, which have the simplest system configuration and the highest sensitivity among them. Our group developed a SPR biosensing system and used heterodyne method to detect the interaction between ricin and its antibody *(2)*. However, it is difficult to realize array detection by heterodyne. Interferometry can detect the phase distribution over the whole sensor area, and is appropriate for array detection. We performed array detection based on spatial modulation phase detection (SMPD), and obtained phase distribution of the antibody-array chip and phase–time curves of all sensing units. Experimental results indicate that this technique has a high sensitivity in array detection.

SPR technique can be used to analyze the interactions of a broad variety of biomolecules. Among all biomolecular interaction model systems, antigen–antibody interaction model system is one of the most common and simple one. So we choose rabbit IgG as an antigen and goat anti-rabbit-IgG IgG (as an antibody), a typical model system which can reflect common characteristics of antigen–antibody interaction, to illustrate the SPR biosensing technique.

## 2. Materials

### 2.1. Reagents and Solutions

1. Piranha solution: 7:3 (volume ratio) mixture of concentrated sulfuric acid and 30% hydrogen peroxide.
2. MUA solution: 11-mercapto-undecanoic acid (MUA, Sigma) dissolved in ethanol at 1 mM and stored at room temperature.

3. Activation solution: 1:1 (volume ratio) mixture of *N*-hydroxy succinimide (NHS, 0.1 M, Sigma) solution and fresh 1-ethyl-3-[3-dimethylaminopropyl]carbodiimide (EDC, 0.4 M, Sigma) solution (*see* **Note 1**).
4. Phosphate buffered saline (PBS) solution: 8 mM $Na_2HPO_4$, 1.5 mM $KH_2PO_4$, 27 mM KCl, and 1.37 M NaCl in high-purity $H_2O$, pH 7.4.
5. Regeneration solution: 0.2 M glycine, pH adjusted to 2.0 with hydrochloric acid.
6. Rabbit IgG solution (Biodee, CN): dissolved in PBS at 1 mg/mL.
7. Goat anti-rabbit-IgG IgG solution (Biodee, CN): dissolved in PBS at 1 mg/mL.
8. Bovine serum albumin (BSA, Amresco) solution: dissolved in PBS at 10 mg/mL.
9. Diiodomethane ($CH_2I_2$, Sigma): used as the refractive index oil, stored in the dark.

### 2.2. Sensing Chip

1. The sensing chip is made of ZF5 glass, the same material as the triangle prism in the Kretschmann configuration.
2. The chip has a size of 12 mm × 12 mm × 1.2 mm, with both surfaces polished (*see* **Note 2**).
3. A chromium (Cr) layer with a thickness of 2 nm is evaporated onto one surface of the chip, at a speed of 0.1 nm/s, in $5 \times 10^{-3}$ Pa vacuum (*see* **Note 3**).
4. A 40-nm gold (Au) layer is evaporated onto the chip surface with predeposition of Cr, at a speed of 0.1 nm/s, in $5 \times 10^{-3}$ Pa vacuum (*see* **Note 4**).
5. Chips are stored in airtight container, protected from dirt and moisture.

### 2.3. Preparation of Antibody Array Chip

1. Before use, the gold surface of the chip should be cleaned thoroughly. First, the chip is dipped in Piranha solution for 5 min, rinsed by pure water, and blown dry. Then it is cleaned ultrasonically in ethanol for 5 min.
2. Immerse the chip in MUA solution over 24 h to form a carboxyl terminated self-assembled monolayer on the gold surface. Then rinse the chip by pure water and blow it dry.
3. Carboxyl groups on the gold surface are activated by immersing the chip in the activation solution for 30 min before they can immobilize antibody molecules. Rinse the chip by pure water and blow it dry.
4. Rabbit IgG solution (1 mg/mL) is manually spotted on the activated carboxyl terminated surface by a pipette. A 2 × 2

array of rabbit IgG spots is fabricated, with spot diameters of about 1 mm. The antibody array chip is incubated at 35°C for 30 min and rinsed by PBS solution thoroughly.

5. The chip is immersed in BSA solution (10 mg/mL) at 35°C for 30 min to block residual activated carboxyl groups, and rinsed by PBS thoroughly.
6. The antibody array chip is glued to the flow cell.
7. Fill the flow cell with PBS solution to keep the chip surface from becoming dry.

### 2.4. Instrumental Configuration

The configuration of the SPR system is shown in **Fig. 2.1**, which can be divided into three parts: the incident arm, the SPR sensing configuration, and the reflective arm.

The incident arm consists of the following (numbers correspond to those in **Fig. 2.1**):

1. A He–Ne laser (200-mm length and 50-mm diameter, purchased from *Qufu Normal University*, CN), which generates frequency-stabilized laser with a beam diameter of about 2 mm, at wavelength of 632.8 nm.
2. A pinhole of 10-μm diameter at the common focus of the lenses in the beam expander, made of aluminum.
3. A beam expander that contains a microscope objective with the focus length of 4.65 mm (*Daheng, Inc.*, CN, GCO-2105) and a lens with the focus length of 30 mm (*Daheng, Inc.*, CN, GCL-0102).
4. A 1/2 wave plate with the diameter of 25.4 mm (*Daheng, Inc.*, CN, GCL-0606).
5. A rectangular diaphragm that has a size of 12 mm × 12 mm.

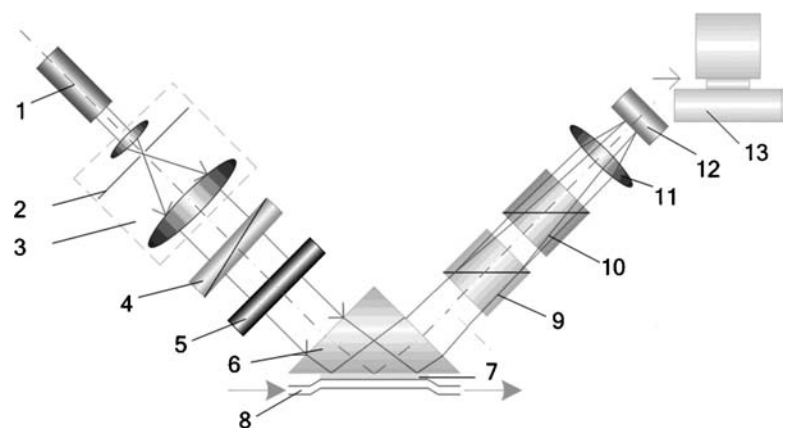


Fig. 1. Configuration of SPR system based on SMPD.

The SPR sensing configuration consists of the following:

6. A Kretschmann prism with an equiangular triangle section and three 20 mm × 12 mm side faces, made of ZF5 glass, whose refractive index is 1.740.
7. A sensing chip (details in **Subheading 2.2.2**).
8. A flow cell (details in **Subheading 2.3.3**).

The reflective arm consists of the following:

9. A Wollaston prism that has a size of 12 mm × 12 mm × 12 mm and a splitting angle of 0.3° (*Qufu Normal University*, CN, LSP-03).
10. A polarizing prism that has a size of 10 mm × 10 mm × 27 mm (*Qufu Normal University*, CN, LGP-01).
11. An imaging lens with focal length of 200 mm and diameter of 38.1 mm (*Daheng, Inc.*, CN, GCL-0101).
12. A 1392 × 1040 CCD camera with 4.65 μm × 4.65 μm pixels, which is connected to the computer through a PCI interface (*Roper Scientific, Inc.*, US, PHOTOMETRICS CoolSNAP *cf*).
13. A computer.

## 3. Methods

### *3.1. SPR Biosensing Based on Phase Detection*

#### *3.1.1. Principle of SMPD*

When SPR occurs, phase of p-polarized light varies abruptly against the refractive index near the gold surface (shown in **Fig. 2.2**), while phase of s-polarized light remains approximately constant. Hence, it provides an approach to measuring the phase change of p-polarized light by using s-polarized light as the reference.

Phase difference between the two light components can not be measured directly. But after passing through a polarizer, their phase difference is connected with the light intensity, defined as:

$$I = I_1 + I_2 \cos(\varphi),$$

where $I$ is the intensity of interference light, $I_1$ and $I_2$ are determined by the intensities of the p-polarized light and the s-polarized light, and $\varphi$ is their phase difference. Since $I_1$ and $I_2$ are unknown, $\varphi$ cannot be obtained by just detecting $I$.

In SPR system based on SMPD, the Kretschmann configuration *(3)* is employed. The Kretschmann configuration is the simplest method to excite SPR and has been widely used in commercialized and laboratory SPR systems, shown in **Fig. 2.3**. In SMPD, the core optical element is a Wollaston prism, splitting the p-polarized component and s-polarized component of the reflected light by a small angle. After passing through a polarizer,

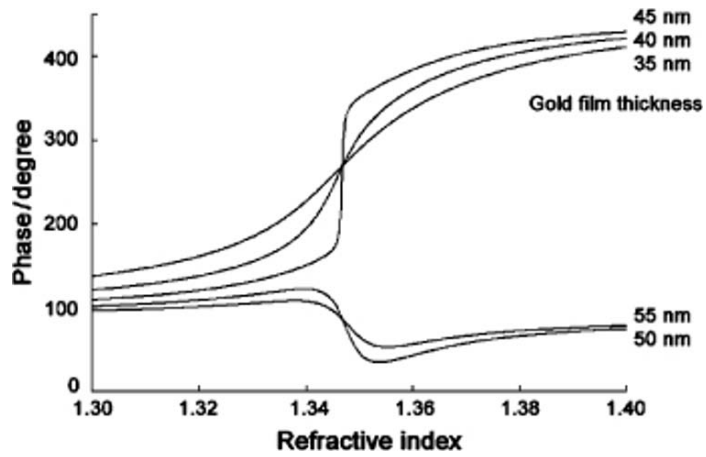


Fig. 2. Phase of p-polarized light against refractive index on SPR sensor surface at different gold film thicknesses. The light wavelength is 632.8 nm. The prism's dielectric constant is 3.08 and the gold's dielectric constant is –10.92 + 1.49*i*.

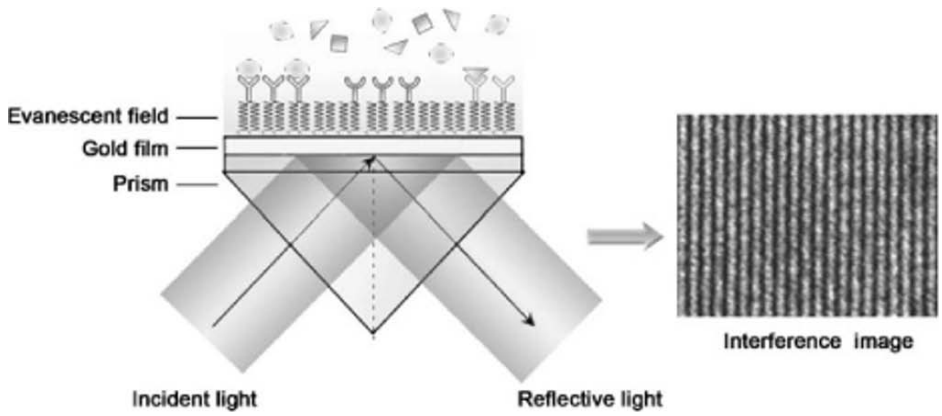


Fig. 3. The Kretschmann configuration and interference image in SPR system based on SMPD. The reflected light passes through a Wollaston prism and a polarizing prism and forms interference stripes on screen.

the two light components interfere with each other and form interference stripes on screen (*see* **Fig. 2.3**), whose intensity is determined by:

$$I(x,y) = I_1 + I_2 \cos[\varphi(x,y) + fx],$$

where $f$ is spatial frequency of the stripes (*see* **Note 5**), $x$ and $y$ are rectangular coordinates on the screen. Collecting the interference images by a CCD camera and processing them with algorithms, phase distribution can be obtained. Several algorithms can be used to calculate the phase difference, such as sinusoidal fitting, correlation, and Fourier transform process (FTP). FTP

gives spatially resolved phase distribution and is appropriate to SPR array detection *(4)*.

### *3.1.2. SMPD Applied to SPR Biosensing*

Biomolecular interaction is the biomolecules' adsorption or desorption to the chip surface, which leads to the change in surface mass density on the chip surface. In fact, surface mass density determines the refractive index. In SPR biosensing, phase of the reflected light is extremely sensitive to the refractive index on the chip surface, which implies that it is sensitive to the biomolecular interaction taking place on the sensor surface. Because of the spatial resolved ability of SMPD in detecting phase distribution, different biomolecules can be analyzed on one chip at the same time.

**Figure 2.4** shows how SMPD is applied to SPR array detection of biomolecular interaction. Several different biomolecules are immobilized on a sensing chip. In SMPD, biomolecules' adsorption or desorption to the chip surface leads to change in refractive index and thereby displacement of the interference

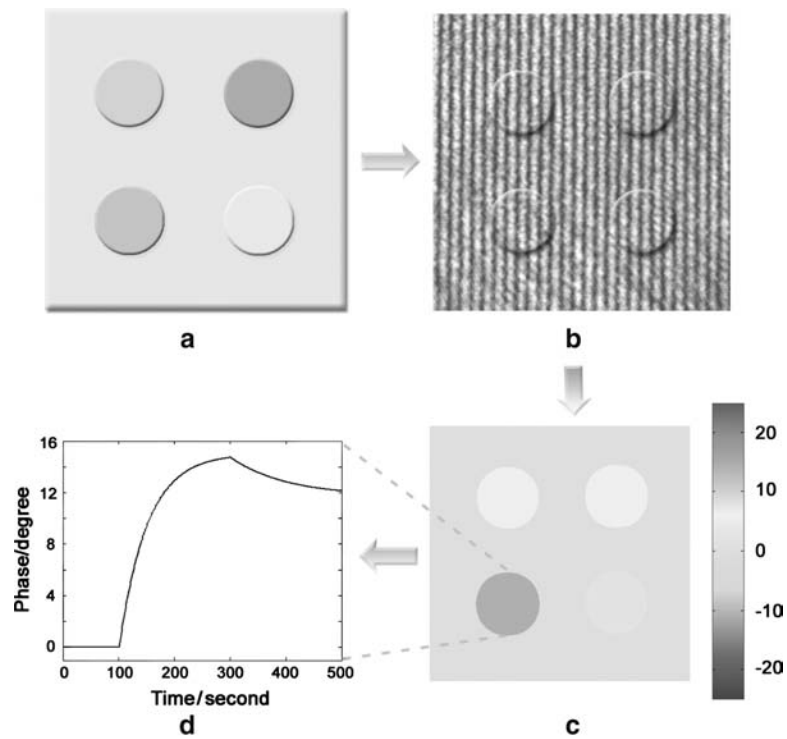


Fig. 4. The principle of SPR biosensing based on SMPD: (**a**) Four different samples are spotted on a chip. (**b**) Biomolecular interaction leads to displacement of interference stripes. (**c**) Change in phase distribution is calculated by algorithms, giving direct positive and negative results. (**d**) Phase–time curve of a sample is obtained, which records the whole process of the sample interacting with the analyte.

stripes. Change in phase distribution caused by biomolecular interaction can be calculated by algorithms. It gives direct results whether there is something binding to or dissociating from the chip surface. Continuously detecting the phase change, the whole process of biomolecular interaction can be recorded in the form of phase change, based on which we can make kinetic analysis and get kinetic parameters.

#### 3.1.3. Optics

Functions of the three parts are as follows: the incident arm generates expanded and collimated monochromatic light beam, the SPR sensing configuration excites SPR and provides a place for biomolecular interaction, and the reflective arm introduces spatial interference and collects image data.

In the incident arm, polarized light from the He–Ne laser 1 is expanded and collimated by the beam expander 3, and filtered by the pinhole 2. The intensity ratio of p-polarized and s-polarized components of the light is adjusted by rotating the ½ wave plate 4. The rectangular diaphragm 5 makes the beam's cross section become a rectangular shape. The light beam is projected into the Kretschmann prism to excite SPR, illuminates the sensing chip 7, and is reflected at the glass–gold interface. To eliminate the air gap between the Kretschmann prism 6 and the sensing chip 7, a kind of matching oil ($CH_2I_2$, diiodomethane) having the same refractive index as the prism 6 is filled in the interface. The reflected light contains information of biomolecular interaction. In the reflective arm, the Wollaston prism 9 and the polarizing prism 10 cooperate to generate interference between p-polarized light and s-polarized light. The interference pattern is imaged onto the CCD camera 12 by the imaging lens 1. The images are collected and sent to the computer 13 for processing and analysis.

When SPR is excited, biomolecular interaction, such as antigen–antibody interaction on the sensing chip 7, leads to great change in the phase of the reflected light. Thus, the SPR interference pattern, which is determined by phase distribution of the reflected light, changes correspondingly to the biomolecular interaction. By collecting the interference images by the CCD camera 13 and processing the data of gray values in the computer 14, we can get quantitative and time-resolved information of biomolecular interaction.

### 3.2. Mounting and Adjusting the Optic System

**Figure 2.5** shows the photo of the optical system.

1. Scribe the base and draw lines parallel to the optic axis, one in the incident arm and the other in the reflective arm.
2. Mount the laser 1 to the base. Ensure that the light beam is parallel to the optical axis (*see* **Note 6**).
3. Mount the pinhole 2 and the expander 3. Adjust the distance between the pinhole 2 and the microscope objective in the

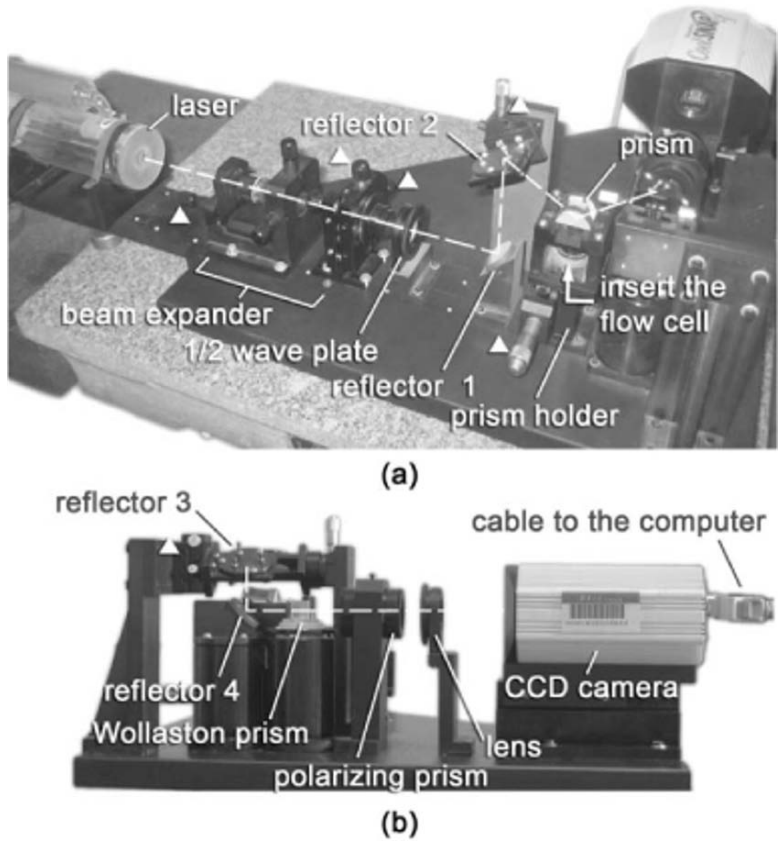


Fig. 5. Photos of the optical system: (**a**) The incident arm: The dashed line is part of the optical axis. Five white triangles indicate the adjusting screws 1–5 from left to right, respectively. The pinhole within the beam expander and the rectangular diaphragm is adhered to ½ the wave plate so that they are not marked in the picture. (**b**) The reflective arm: The dashed line is part of the optical axis. The white triangle indicates the adjusting screw 6.

expander 3 by the adjusting screw 1, until the light beam from the expander 3 has a maximum light intensity and a uniform intensity distribution.

4. Adjust the orientation and the position of the lens in the expander 3 by the adjusting screws 2 and 3 and make the light beam a collimated beam and parallel to the optical axis.
5. Mount the ½ wave plate 4 and two reflectors (the orientation of reflector 1 is fixed and that of the reflector 2 can be adjusted).
6. Mount the prism holder to the base.
7. Mount two reflectors (one reflector's orientation is fixed and that of the other's can be adjusted) in the reflective arm, and rotate the reflector 4 to make the light beam parallel to the optical axis.
8. Mount the Wollaston prism 9, the polarizing prism 10, the imaging lens 11, and the CCD camera 12 to the base according

to the screw holes in the base. Connect the CCD camera to the computer with cables.

### 3.3. The Fluidic System

1. The fluidic system consists of an injecting system, a four-way valve, a flow cell, and a tubing system, as shown in **Fig. 2.6** (*see* **Note 7**).
2. The injecting system involves a homemade injecting device and four syringes (two 10-mL syringes and two 2.5-mL syringes, only three of them are used in the experiments).
3. The four-way valve is made of polymethyl methacrylate (PMMA) with three inlets and an outlet.
4. The structure of the flow cell in shown in **Fig. 2.7**. The flow cell is made up of two parts: a flat plate and a plate with flow channels processed in it. The two parts of the flow cell are made of PMMA and adhered together by $CHCl_3$ (trichloromethane). The flow cell has a volume of 30 µL.

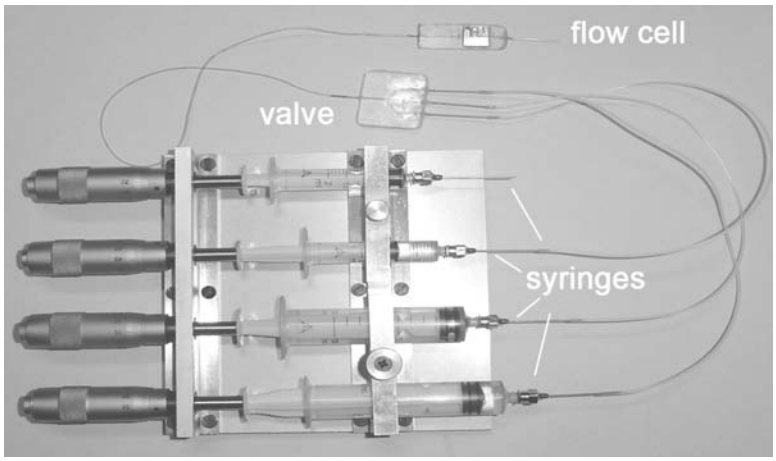


Fig. 6. A photo of the fluidic system.

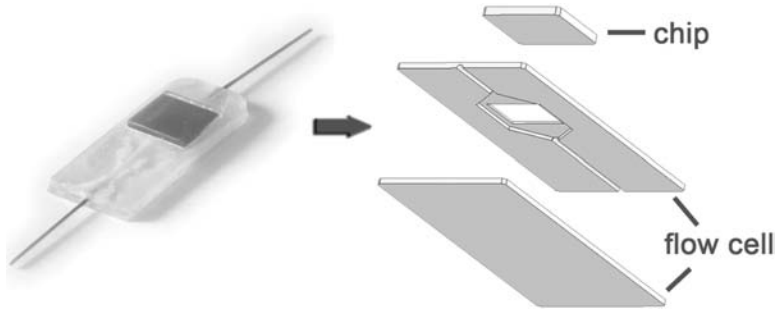


Fig. 7. The flow cell. The whole flow cell consists of three parts: the chip, the upper part of the flow cell (a flat PMMA plate), and the lower part of the flow cell (a PMMA plate with channels processed in it).

5. The chip is adhered to the flow cell by 502glue, with the gold surface toward the inside of the cell.
6. The tubing system is made of polytetrafluoroethylene (PTFE) tube with the inner diameter of 0.7 mm.

### 3.4. Experimental Procedures

1. Before experiments, fill the syringes with PBS solution, goat anti-rabbit-IgG IgG solution (1 mg/mL), and regeneration solution, respectively.
2. Clean the glass surface of the sensing chip with ethanol. Add about 2-μL diiodomethane onto the glass surface of the chip and mount the flow cell to the Kretschmann configuration (*see* **Note 8**).
3. Rotate the reflector 2 by the adjusting screw 4 in front of the prism to adjust the incident angle to excite SPR and observe the intensity of the reflected light by CCD. The resonant angle is slightly lower than 60°, corresponding to the minimum intensity of the reflected light.
4. Adjust the prism height by the adjusting screw 5 in the prism holder and rotate the reflector 4 by the adjusting screw 6 corresponding to the adjustment to the incident angle.
5. Rotate the polarizers and adjust the exposure time of the CCD to get interference image with good contrast.
6. Start to collect interference images at a speed of 0.5 frame/s.
7. When starting to collect images, inject PBS solution into the flow cell continuously, lasting 80 s at a flow rate of 200 μL/min.
8. Inject goat anti-rabbit-IgG IgG solution slowly to form antigen–antibody complex, lasting 300 s at a flow rate of 200 μL/min.
9. Inject regeneration solution to dissociate the antigen–antibody complex, lasting 100 s at a flow rate of 200 μL/min.
10. Inject PBS solution for 120 s at a flow rate of 200 μL/min.
11. Stop collecting images and save data in computer.

### 3.5. Signal Processing and Result Analysis

1. Use FTP algorithm to calculate the phase distribution of the reflected light (*see* **Note 9**).
2. Subtract the phase distribution at $t$ = 1 s from the phase distribution at $t$ = 380 s to get the phase change caused by goat anti-rabbit-IgG IgG binding to rabbit IgG, shown in **Fig. 2.8** (*see* **Note 10**). In **Fig. 2.8**, four white regions can be distinguished obviously, representing four rabbit IgG spots. The color bar has the unit of degree. Higher phase change value indicates that there are more molecules binding to the chip surface. Maximum phase change is higher than 12°,

while background (BSA, dark region) displays fairly low noise level, about 2–3°.

3. Calculate the phase–time curves of rabbit IgG spots and background (*see* **Note 11**). **Figure 2.8** shows the phase distribution after rabbit IgG binds to goat anti-rabbit-IgG IgG, with four sample areas S1, S2, S3, and S4 (rabbit IgG) and two reference areas R1 and R2 (BSA) (*see* **Note 12**).
4. Phase–time curves of sample area A and background area B are shown in **Fig. 2.9a**. Background signal is generated by bulk refractive change, nonspecific binding, and high-frequency noise. Directly subtracting the background signal from the sample signal, phase change generated by bulk refractive change and nonspecific binding is completely removed from the signal of sample area, and high-frequency noise can also be eliminated to a great extent. The phase resolution of the system is higher than 0.2°, equivalent to $3 \times 10^{-5}$ RIU in refractive index (*see* **Note 13**). **Figure 2.9b** shows the processed signal

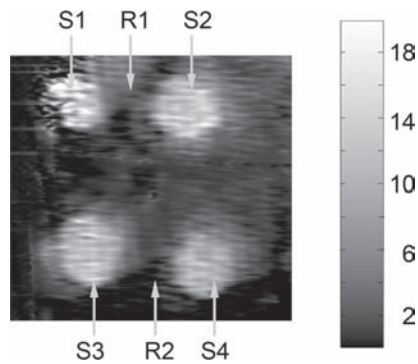


Fig. 8. Phase distribution after rabbit IgG binds to goat anti-rabbit-IgG IgG, with four sample areas S1, S2, S3, and S4 (rabbit IgG) and two reference areas R1 and R2 (BSA).

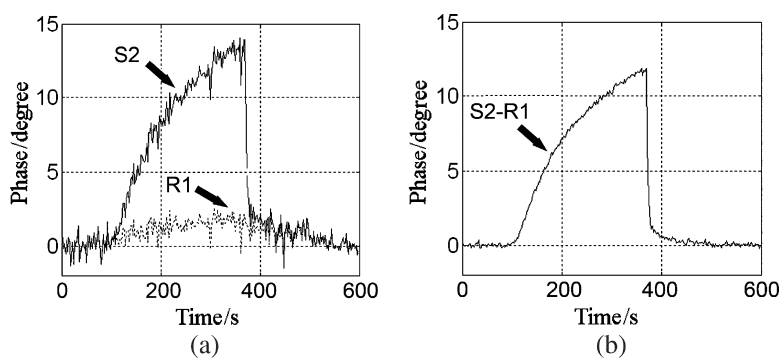


Fig. 9. Phase curves of the sample area S2 (rabbit IgG) and the reference area R1 (BSA): (**a**) Original phase curves. (**b**) Phase curve after background is subtracted.

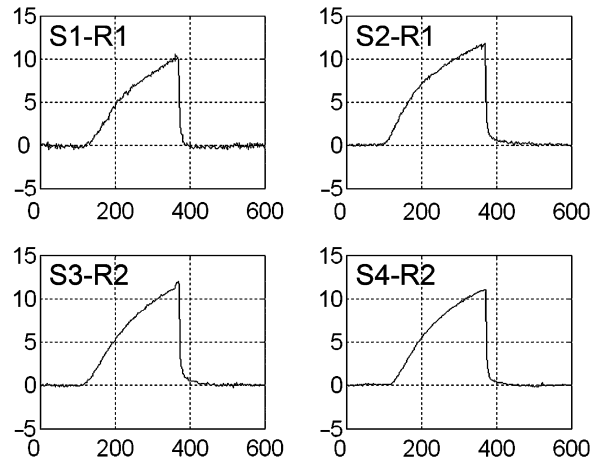


Fig. 10. Curves of sample signals minus background signals.

by subtracting the background signal from the sample signal. From 80 to 380 s, antigen–antibody binding process is revealed clearly by the ascending phase curve, and the phase signal rapidly drops to 0° when regeneration solution is injected.

5. **Figure 2.9** shows the phase–time curves of four sample area minus two reference areas, respectively. In **Fig. 2.10**, *x*-axis is the time (unit: second) and the *y*-axis is the phase change (unit: degree). Curves of these areas vary almost consistently (*see* **Note 14**).
6. As for kinetics analysis, goat anti-rabbit-IgG IgG at a series of concentrations is tested to repeat the above experiment cycle and get a group of phase–time curves. By fitting these curves with proper exponential function, association rate constant, dissociation rate constant, and affinity constant can be obtained.
7. In practical application, a number of different biomolecules can be analyzed at the same time by spotting them onto one chip (*see* **Note 15**).

## 4. Notes

1. EDC powder is stored at –20°C and protected from moisture. Make sure that only fresh solution is used because EDC is moisture sensitive and quickly hydrolyzed in water.
2. Herein *surface* refers in particular to the surface of the chip with size of 12 mm × 12 mm, and the same below.

3. Predepositing a Cr layer makes the gold layer adhere to the chip surface firmly.
4. The thickness of the gold layer is chosen to be 40 nm in order to get a high sensitivity and a large dynamic range *(2)*.
5. The spatial frequency $f$ is the reciprocal of the period of the interference stripes $d$, $f = 1/d$. The period $d$ can be theoretically calculated by equation $d = \alpha / \lambda$, in which $\alpha$ is the splitting angle of the Wollaston prism and $\lambda$ is the light wavelength. In this system, $\alpha$ is 0.3° and $\lambda$ is 632.8 nm. So the calculated period of the interference pattern is 120.9 μm, equivalent to the width of 26.0 pixels in a line on the CCD camera.

   The experimental period value $d$ can also be obtained by fitting the interference pattern in horizontal direction with ideal sinusoidal function, and the fitted period value is about 24.9 pixels, which is consistent with the theoretically calculated value. The tiny difference between the theoretically calculated value and experimentally obtained value may originate from the manufacturing error in the Wollaston prism's splitting angle.
6. Herein *parallel to the optical axis* means parallel to the base and simultaneously parallel to the scribed line on the base. All parts and components are mounted to the base through screws holes in the base.
7. In order to get a better repeatability of the flow rate and automatically handle the fluid injection, commercialized automatic injecting system can be substituted. Commercialized valves and tubes can also be found.
8. Cleanness of the glass surface is very important since any impurity even moisture remaining between the prism and the chip could intervene in the optical path and influence the accuracy of the results. It is also necessary to eliminate the air bubble between the prism and the chip.
9. The spatial frequency of the interference stripes is obtained by fitting the gray values with standard sinusoidal curve, which is consistent with the theoretically calculated spatial frequency. Parameters in the algorithm such as frequency shift and cut frequency are determined according to the fitted spatial frequency value.
10. The phase distribution remains invariable from $t = 1$ to 80 s. Antigen–antibody complex begins to form at $t = 80$ s and ends at $t = 380$ s. Only phase change tells the biomolecular binding or dissociation. Absolute phase value makes no sense since it is determined by the light beam's inherent phase distribution and the optical system.
11. The phase–time curve is calculated by averaging the phase values in an area of 100 × 100 pixels in the sample area or background area. In practice, the size of the averaged area is

determined by the spot size when fabricating the array chip. The larger the area used to calculate the average value, the higher precision will be obtained.

12. It is better to choose a background area that is close to the sample area in respect that it gives better noise reduction performance when subtracting the background signal from the sample signal.
13. The phase resolution of the system is determined by NaCl solution experiments in which NaCl solution of different concentrations is tested. The lowest concentration of the NaCl solution that can be detected is 0.02%, which generates 0.2° phase change. In form of refractive index, the detection limit is as low as $3 \times 10^{-5}$ RIU. As in protein–protein interaction analysis, the system can detect 3 ng/cm$^2$ of absorbed protein on the chip surface.
14. Curve S1-R1 shows a higher noise level comparative to the other curves, which is generated by optical noise and can be avoided by system improvement.
15. In SMPD, several periods of interference stripes are needed to calculate the phase change. Thereby, there is a limit to the number of biomolecules spotted onto one chip, typically not more than 20.

## Acknowledgments

This research is supported by the National Natural Science Foundation of China (NSFC, Grant No. 30727001) and the Specialized Research Fund for the Doctoral Program of Higher Education (SRFDP, Grant No. 20050003056).

### References

1. Yu X., Wang D., and Yan Z. (2003) Simulation and analysis of surface plasmon resonance biosensor based on phase detection. *Sensors and Actuators B* 91, 285–290
2. Yu X., Zhao L., Jiang H., Wang H., Yin C., and Zhu S. (2001) Immunosensor based on optical heterodyne phase detection. *Sensors and Actuators B* 76, 199–202
3. Kretschmann E., and Raether H. (1968) Radiative decay of non-radiative surface plasmons excited by light. *Zeitschrift fur Naturforschung* 23A 2135–2136
4. Liu J., Ding X., Yu X., and Wang D. (2005) Data analysis of surface plasmon resonance biosensor based on phase detection. *Sensors and Actuators B* 108, 778–783